Three new co-crystals of hydroquinone: crystal structures and Hirshfeld surface analysis of intermolecular interactions†

Henrik F. Clausen,[a] Marie S. Chevallier,[a] Mark A. Spackman[b] and Bo B. Iversen*[a]

Received (in Montpellier, France) 7th September 2009, Accepted 30th October 2009
First published as an Advance Article on the web 15th December 2009
DOI: 10.1039/b9nj00463g

Hydroquinone (benzene-1,4-diol or quinol) is reported here to form co-crystals in different ratios with propan-2-ol, *N*,*N*-dimethylacetamide (DMA) and *N*,*N*-diethylformamide (DEF). Investigation of intermolecular interactions and crystal packing *via* Hirshfeld surface analysis reveals that more than two-thirds of the close contacts are associated with relatively weak H···H, C···H and H···C interactions. The use of Hirshfeld surfaces in combination with fingerprint plots demonstrates that these weak interactions are important for both local packing and crystal packing. The complexes highlight the way in which electrostatic complementarity to a large extent governs the hydrogen bonding pattern in molecular crystals.

Introduction

Although supramolecular chemistry underpins the design and development of materials for a vast number of applications (*e.g.*, sensors, nonlinear optics, switches *etc.*),[1] it is striking that the fundamental chemical interactions governing even the simplest self-assembly processes are not well understood.[2] In order to understand self-assembly at a fundamental level it is necessary to obtain atomic-level information, and molecular crystals are the ideal supramolecular entities.[3] However, one of the big challenges in studying molecular crystals is complexity. A typical molecular crystal will have thousands of superimposed intermolecular interactions, which all contribute to the cohesive energy of the solid. A detailed understanding of intermolecular interactions presently relies predominantly on the tabulation of interatomic distances and geometries, an approach that is painstaking to the researcher, very difficult to interpret for the reader, and by its very nature lacking a great deal of key structural information. As such, the important step of analyzing how molecules interact with their direct environment presents a considerable barrier in the understanding and communication of structure and its relationship to properties. Hirshfeld surface based tools represent a novel approach to this problem.[4–6] The central element in this method is the derivation of the Hirshfeld surface—an immediately interpretable visualization of a molecule within its environment—and the decomposition of this surface to provide a 'molecular fingerprint'—a directly accessible 2D map that provides the full distribution of interactions. The former, in addition to being an invaluable visualization tool, provides a basis for quantitative analysis of molecular properties for comparison with bulk measurement. The latter allows convenient comparison between molecules in different environments. Analysis of intermolecular interactions using Hirshfeld surface-based tools represents a major advance in enabling supramolecular chemists and crystal engineers to gain insight into crystal packing behaviour.

The compounds reported here, Scheme 1, form part of a general program to study intermolecular interactions, with a special focus on crystalline host–guest systems such as the β-hydroquinone clathrates.[7] This system has the ability of encaging a variety of small molecules, such as CO_2, CH_3OH and CH_3CN.[8–10] The host β-hydroquinone structure can be synthesized without any enclathrated solvent molecules, and this "empty" system can be used as a reference system for physical property measurements of the clathrates.[11] In an attempt to obtain the guest free reference structure, hydroquinone (HQ) was dissolved in the relatively bulky solvent propan-2-ol. Slow evaporation of the solvent resulted in a mixture of crystalline phases, which were determined to be the α-form,[12] the guest free β-form and the novel co-crystal **1**.

Attempts to obtain new clathrate compounds resulted in two further new co-crystals, **2** and **3**, which also have been

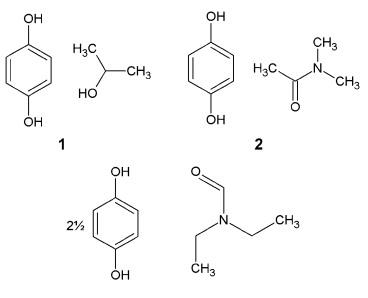

Scheme 1

[a] *Centre for Material Crystallography, Department of Chemistry, and Interdisciplinary Nanoscience Center iNANO, Aarhus University, Langelandsgade 140, DK-8000 Aarhus C, Denmark. E-mail: bo@chem.au.dk; Fax: +45 8619 6199; Tel: +45 8942 3969*
[b] *School of Biomedical, Biomolecular and Chemical Sciences, University of Western Australia, 35 Stirling Hwy, Crawley, WA 6009, Australia*

† Electronic supplementary information (ESI) available: Bond lengths, bond angles, d_{norm} plotted on Hirshfeld surfaces, electrostatic potential plotted on both Hirshfeld surfaces and electron density isosurfaces, fingerprint plots and table of dipole moments for all molecules in the three solvates. CCDC reference numbers 692266–692268. For ESI and crystallographic data in CIF or other electronic format see DOI: 10.1039/b9nj00463g

obtained by slow evaporation at room temperature from a solution of HQ and the solvents, *N*,*N*-dimethylacetamide (DMA) and *N*,*N*-diethylformamide (DEF), respectively. We report here the crystal structures of the three new co-crystals along with an investigation of the close intermolecular contacts between the molecules *via* Hirshfeld surface analysis in order to reveal subtle differences and similarities of the HQ molecules in the three crystal structures. Local packing and related close contacts are examined by breakdown of fingerprint plots.[13–15] An investigation of HQ co-crystal structures deposited in the Cambridge Structural Database has also been carried out.

Results and discussion

Crystal structures

In all cases slow evaporation of solvent from a HQ solution provided single crystals suitable for X-ray diffraction experiments. The crystal structure of **1** consists of hydrogen bonded units of HQ and propan-2-ol in a ratio of 1 : 1 (Fig. 1).

There are two unique HQ molecules in the unit cell (two half hydroquinone molecules each lying about independent inversion centres), and both are in a *trans*-conformation, with the hydroxyl groups of each acting as both acceptor and donor generating a hexagonal chair-conformation of hydrogen bonded hydroxyl groups similar to the carbon skeleton ring in cyclohexane. The hexagons are connected by the aromatic benzene rings thus generating a two dimensional hydrogen bonded layer. Translation along the *b*- or *c*-axis generates a new hydrogen bonded layer. The distance between these layers is greater than 2.37 Å (minimum H–H distance), and hence no close contacts are observed between them. Therefore only weak interactions can be present between the discrete corrugated layers which interdigitate.

Co-crystal **2** crystallizes in a 1 : 1 HQ : DMA ratio, and although the crystal quality was poor, a data set of sufficient quality was still able to be collected. In **2** hydrogen bonded HQ molecules form a continuous one-dimensional chain through the structure following the diagonals of the *ab* plane. Fig. 2 illustrates the hydrogen bonding connectivity of **2**. No close contacts are observed between the discrete one-dimensional chains as the interchain distance is above 2.44 Å. These chains interdigitate, and thus the three dimensional structure of **2** is also dominated by weak interactions. Interestingly, the hydroxyl groups of the HQ molecules point in the same direction generating a *cis*-conformation of the HQ molecule. One of the hydroxyl groups acts only as donor (O1–H1), while the other is both donor and acceptor (O4–H4).

The structure of **3** differs significantly from **1** and **2**, as the HQ : DEF ratio is 5 : 2, with four unique HQ molecules in the unit cell (three half hydroquinone molecules each lying about independent inversion centres, and one hydroquinone molecule and one DEF molecule in general positions). Three of the HQ molecules (HQa(**3**), HQb(**3**), HQc(**3**)) are connected through hydrogen bonds to form a partial hexagon, which terminates at the DEF molecule (Fig. 3). The remaining HQ molecule (HQd(**3**)) is hydrogen bonded to two DEF units,

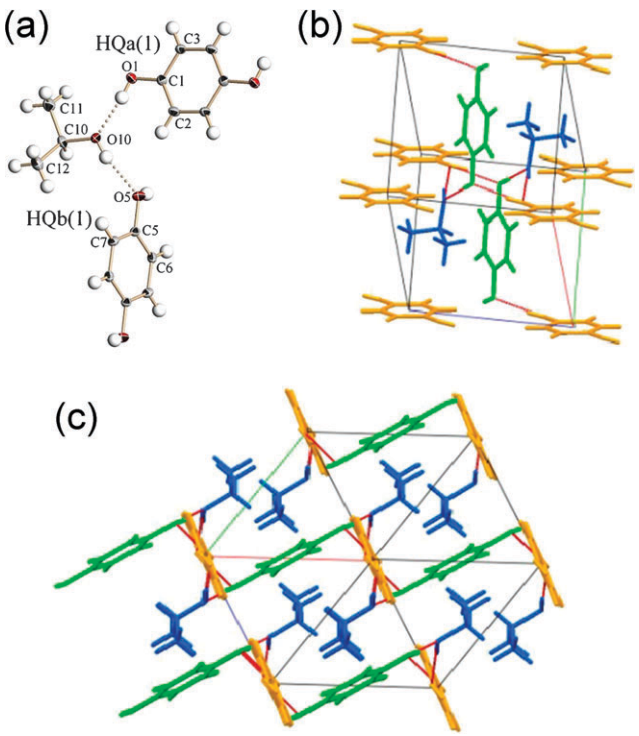

Fig. 1 (a) The structure of **1**, with labelling of atoms in the asymmetric unit. Displacement ellipsoids are drawn at the 50% probability level. (b) The unit cell of **1** visualizing the hydrogen bonded hexagon illustrated by the red lines. (c) The packing of **1** illustrating the discrete corrugated layers which interdigitate. The blue molecules are propan-2-ol, the green are HQa(**1**), and the yellow molecules are HQb(**1**).

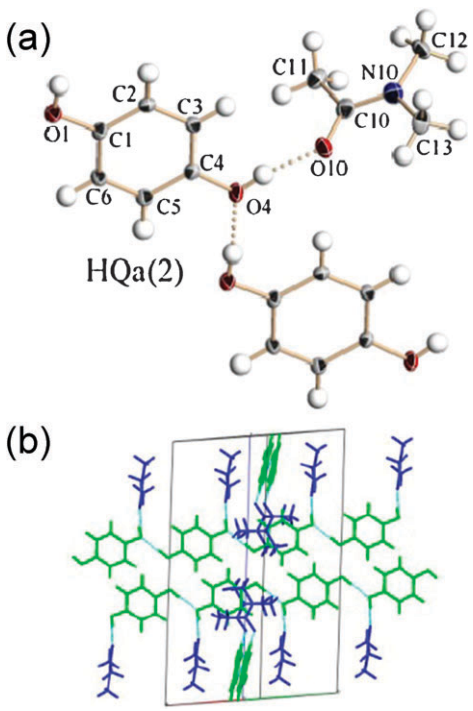

Fig. 2 (a) The structure of **2** with labelling of atoms in the asymmetric unit. Displacement ellipsoids are drawn at the 50% probability level. (b) The packing of **2** viewed along the diagonal of the *ab*-plane. Blue molecules are DMA, and the green molecules are HQa(**2**).

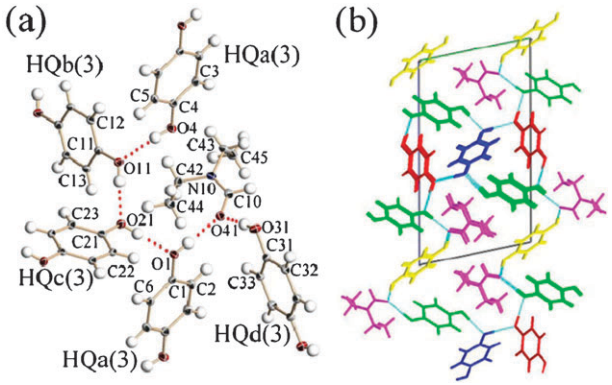

Fig. 3 (a) The structure of **3** with labelling of atoms in the asymmetric unit. Displacement ellipsoids are drawn at the 50% probability level. (b) The packing of **3** viewed along the channels in the structure and the *a*-axis of the unit cell. Pink molecules are DEF, green are HQa(**3**), blue molecules are HQb(**3**), red are HQc(**3**), and the yellow molecules are HQd(**3**).

generating a three dimensional network. The hydroxyl groups of the HQ molecules are all in the *trans*-conformation, but some act only as donor (O4–H4 and O31–H31) whilst others are both donors and acceptors. The hydrogen bonding pattern (HQa(**3**), HQb(**3**) and HQc(**3**)) partially resembles the hydrogen bonded hexagon observed in the *β*-hydroquinone clathrates, where small molecules fit snugly inside the cavities generated by HQ molecules.[10] In **3** a larger cavity is created by the HQ molecules, with two DEF molecules related by inversion symmetry inside. Above and below the cavity, DEF molecules are also situated, thus creating a 3-dimensional structure with channels along the *a*-axis of the unit cell (Fig. 3).

The large number of unique HQ molecules in the structure of **3** is particularly unusual, with a single precedent in the CSD,[16] and only one structure has been reported with a greater number of unique HQ molecules.[17]

No significant differences in bond lengths and angles are observed for the aromatic systems of the seven unique HQ molecules in these three crystal structures. The angle between hydroxyl oxygen atom and aromatic system is changed by ~2.5° from 120° to accommodate the hydrogen atom in the plane of the aromatic ring, and the *cis*-conformation differs from the remaining hydroquinone molecules as the hydroxyl groups are tilted in the same direction. The hydrogen bonding pattern of the HQ molecules varies between the different co-crystals, but all close contacts are dominated by hydrogen bonding interactions. Only the structure of **3** can be described entirely by these interactions, and hence in **1** and **2** not only the short H···O contacts are important, but also the more subtle H···H and C···H contacts.

Hirshfeld surface analysis

Each molecule in the asymmetric unit of a given crystal structure will have a unique Hirshfeld surface, and hence a direct comparison can be made between HQ molecules in different environments. Hirshfeld surfaces provide a three-dimensional picture of close contacts in a crystal, and these contacts can be summarized in a fingerprint plot.[4] The distance from the Hirshfeld surface to the nearest atoms

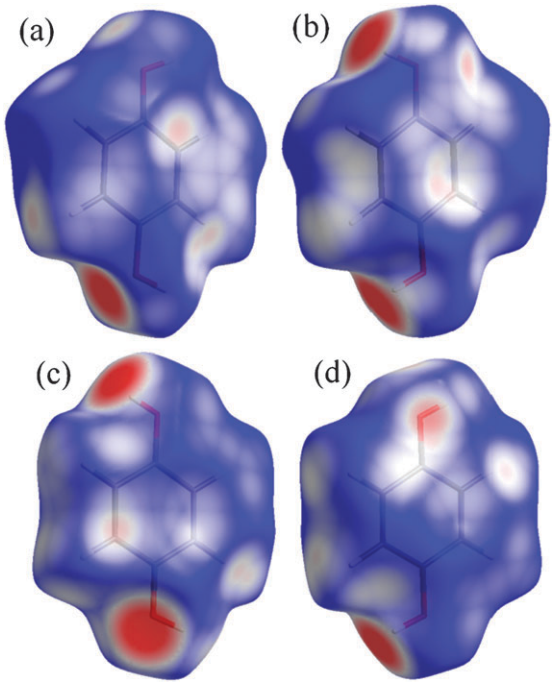

Fig. 4 (a) Front and (b) back views of d_{norm} mapped on the Hirshfeld surface of HQa(**2**) in the *cis*-conformation, and (c) front and (d) back views of HQa(**3**) in the *trans*-conformations. d_{norm} ranges from –0.5 Å (blue) to 0.5 Å (red).

outside and inside the surface are characterized by the quantities d_e and d_i, respectively, and the normalized contact distance based on these, $d_{norm} = (d_i - r_i^{vdW})/r_i^{vdW} + (d_e - r_e^{vdW})/r_e^{vdW})$, is symmetric in d_e and d_i, with r_i^{vdW} and r_e^{vdW} being the van der Waals radii of the atoms. When d_{norm} is mapped on the Hirshfeld surface, close intermolecular distances are characterized by two identically coloured regions, even if these occur on different molecules. The surface mapping of this function highlights the donor and acceptor equally and it is therefore a powerful tool for analyzing intermolecular interactions, such as hydrogen bonds and the weaker C···H contacts (C–H···π).

The Hirshfeld surfaces of HQ molecules of the three co-crystals were analyzed to clarify the nature of the intermolecular interactions. Fig. 4 provides d_{norm} surfaces of the *cis*-conformation of HQa(**2**) and the *trans*-conformation of HQa(**3**). The surfaces are shown as transparent to allow visualization of the orientation and conformation of the hydroxyl groups in the molecules.

As expected, the surfaces in Fig. 4 reveal the close contacts of hydrogen bond donors and acceptors, but other close contacts are also evident. The illustrated molecules were selected due to the different conformations and diversity of the hydroxyl groups as both molecules include a group acting as both donor and acceptor (lower group) and one acting only as a donor (upper group). Not unexpectedly, the closest contacts observed for the HQ molecules are all due to the hydrogen bonding interaction in the form of O···H contacts. Even though the O···H interactions are shortest and most likely strongest, they cover at most one-third of the Hirshfeld surface of the HQ molecules, and hence other weaker

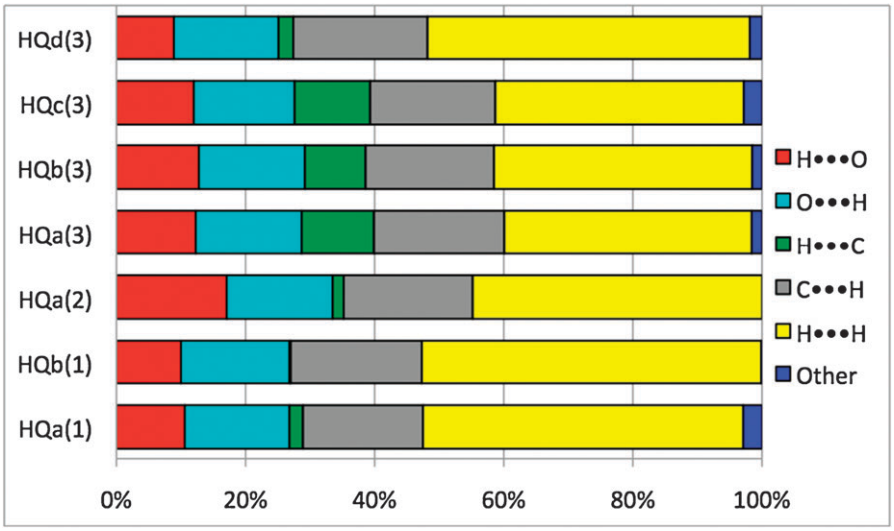

Fig. 5 Close contacts to the Hirshfeld surfaces of HQ molecules in **1**, **2** and **3** broken down into six different basic interaction types: O–H···O hydrogen bonding—both donor (red) and acceptor (cyan); H···C contacts (green); C···H contacts (grey); H···H contacts (yellow); and all other contacts (blue). The notation C···H refers to close contacts between C atoms inside the Hirshfeld surface (*i.e.* belonging to the HQ molecule of interest) and H atoms outside.

interactions cannot be neglected, see Fig. 5. The contact distance of the O···H interactions is the shortest, but as pointed out above only the crystal structure of **3** can be adequately rationalized from the hydrogen bonding interactions alone.

The C···H close contacts are according to Fig. 5 (grey) observed in similar quantity for all HQ molecules in these co-crystals. The directional C···H close contacts that are associated with π···H interaction of a benzene ring with the surrounding molecules, are observed as 'spikes' in the lower right corner of the fingerprint plots at the feature labelled '5' in Fig. 6. Even though the percentage of C···H interaction is approximately the same for all HQ molecules, the fingerprint plot for HQd(**3**) differs as the characteristic feature of the directional interaction is missing, and thus no weak π···H interaction is present for that HQ molecule. Fig. 5 also suggests that HQ molecules with relatively many H···C contacts (green) have fewer H···H contacts (yellow).

Molecules HQa(**3**), HQb(**3**) and HQc(**3**) display significant H···C interactions (*e.g.*, the features labelled '4' in the plot for HQa(**3**) in Fig. 6), and correspond to weak H···π interactions of hydrogen atoms with an adjacent aromatic ring. The molecule HQd(**3**) does not exhibit this type of interaction, and hence does not participate to a significant extent in either H···π or π···H interactions. These interactions of HQ hydrogens with an adjacent aromatic ring are not observed in **1** and **2**, but subtle H···π interactions are present from solvent to HQ. These weak interactions in the structures of **1** and **2** appear to be essential for crystal packing, as no strong interactions are apparent between the layers and chains, respectively. The features labelled '3' in Fig. 6 identify H···O hydrogen donor atoms interacting with oxygen atoms, whereas the acceptor oxygen atoms exhibit similar features, labelled '1' in Fig. 6. The use of Hirshfeld surfaces readily reveals such subtle interactions, and the diversity of the close interactions of HQ in the co-crystals.

The three aromatic systems with pronounced H···C contacts exhibit the smallest molecular volumes as determined by the Hirshfeld surface, see Table 1. Not surprisingly, the HQ molecules with the smaller volumes (HQa(**3**), HQb(**3**), HQc(**3**) and HQd(**3**)) are present in the structure of **3**, which has the highest density of the co-crystals. The H···π interactions discussed above in combination with the smaller volume suggests closer packing of these molecules. The structures with many H···H interactions on the other hand have less dense packing. There are also small differences evident between the HQ molecules in **3**. The volume of HQd(**3**) is larger, correlating with relatively more H···H interactions and less H···C interactions (Fig. 5). The HQd(**3**) molecule does not reveal any H···π or π···H interactions in the fingerprint plots (*e.g.* no 'spikes' characteristic of C···H or H···C interactions). Overall, there are no clear interactions between the aromatic system of HQd(**3**) and the surrounding crystal. As the volume of HQd(**3**) is larger than observed for the other hydroqinone molecules in **3**, and no interaction with the aromatic system is revealed, it can be concluded that the local packing density of HQd(**3**) is smaller.

Using the Hirshfeld surface volumes of each molecular component in the unit cells of the structures, the volume percentage of HQ in the unit cell can be obtained, see Table 1. The volume percentage rises going from the 1-dimensional chains of **2**, through the layered structure of **1** to the 3-dimensional hydrogen bonded structure of **3**. The hydrogen bonding pattern of **3** resembles the pattern observed in the acetonitrile *β*-HQ clathrates, however there the volume percentage of HQ observed in the clathrate structure is far greater at 86%.[10] Even though the structure of **2** has a low volume percentage of HQ compared to **1** and **3**, it is the highest of any HQ co-crystal involving a *cis*-conformer, as these have a tendency to crystallize with large molecules.[18]

Properties can be plotted on the Hirshfeld surface, which is defined by the molecular environment of the molecules.

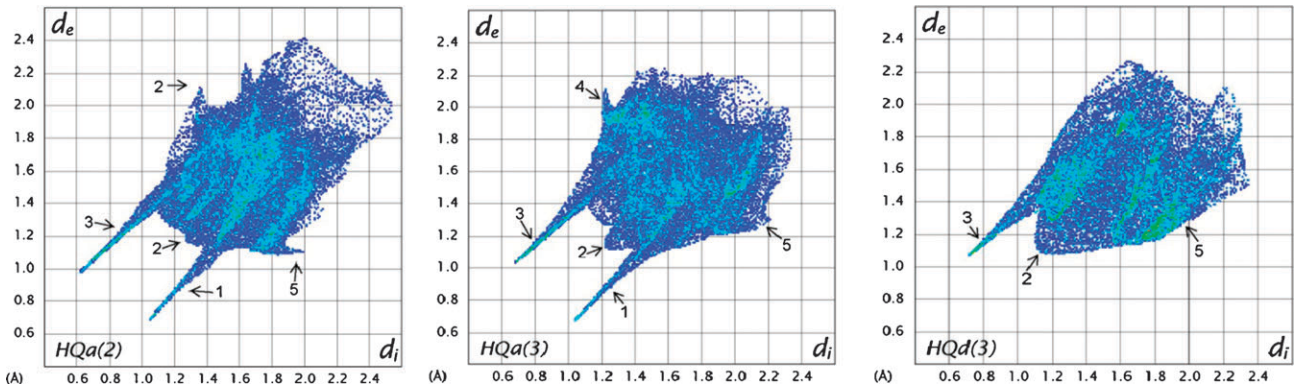

Fig. 6 Fingerprint plots of the HQ molecules HQa(**2**), HQa(**3**) and HQd(**3**). Close contacts are divided into five regions; 1 is O···H, 2 is H···H, 3 is H···O, 4 is H···C and 5 is C···H. Plots for the other molecules are given in the supporting information.†

Table 1 The volumes of the molecules in **1**, **2**, and **3** as determined from the Hirshfeld surfaces

Molecule	Volume/Å^3	Volume/% of unit cell
HQa(**1**)	130.8	57.5
HQb(**1**)	128.6	
Propan-2-ol	96.0	42.5
HQa(**2**)	127.6	50.4
DMA	125.8	49.6
HQa(**3**)	125.3	68.8
HQb(**3**)	124.3	
HQc(**3**)	124.6	
HQd(**3**)	126.7	
DEF	142.3	31.2

Alternatively, properties such as the electrostatic potential can be plotted on molecular electron density isosurfaces. Positive regions of the electrostatic potential preferably interact with complementary negative regions on neighbouring molecules. The range of values of the electrostatic potential mapped on electron density isosurfaces do not differ significantly between the different HQ molecules in these co-crystals (values ranging from 0.089 ± 0.001 to –0.050 ± 0.001 au). Fig. 7 shows that the electrostatic potential is symmetrically distributed about the center of the benzene ring for HQ molecules in the *trans*-conformation. However, the electrostatic potential of the *cis*-conformation is markedly different, as one side of the HQ molecule is clearly more electropositive than the other.

The difference of the charge distribution between the two conformations is also evident in the dipole moments of the HQ molecules: those with *trans*-conformation have a calculated dipole moment close to zero, whereas the *cis*-conformation has a significant moment of 2.73 D,[19] a result close to the experimental value of 2.38(2) D determined by microwave spectroscopy.[20]

The intermolecular interactions in the crystal can be rationalized using the electrostatic potential mapped on the Hirshfeld surfaces, as in Fig. 8.

The poor crystal quality of **2** may possibly be related to the weak long range packing of the one-dimensional chains in this structure. In the structure of **1** the packing of the two dimensional layers is also dominated by weak long range interactions, whereas in **3** the packing can be described by the short

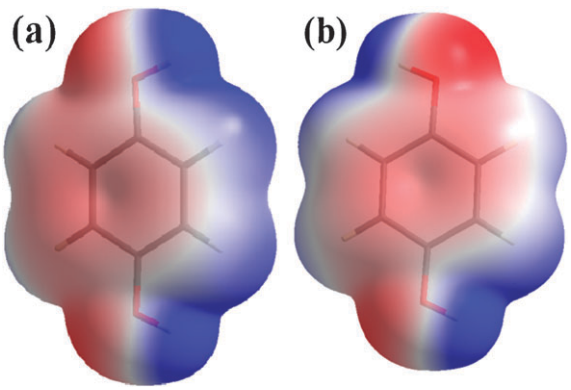

Fig. 7 (a) The electrostatic potential plotted on an isosurface of the electron density of 0.001 e/au^3 of HQ in the *cis*-conformation of **2** and (b) the *trans*-conformations from **3**. Values of the electrostatic potential are plotted from 0.05 au (blue) to –0.05 au (red).

hydrogen bonding contacts. Even though the interactions are weak in **2** there is a striking electrostatic complementarity involved in the packing of the one-dimensional chains, as visualized in Fig. 8. The electronegative regions (red) of the HQ molecule are adjacent to the electropositive (blue) region of the DMA molecules of the neighbouring chain.

Conformations of hydroquinone molecules

HQ is known to co-crystallize with a diverse range of compounds. In the solid state the hydroxyl groups of HQ molecules can adopt either a *trans*- or a *cis*-conformation.

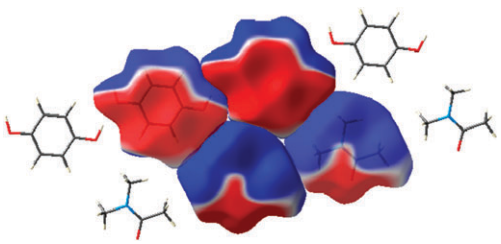

Fig. 8 The electrostatic potential mapped on the Hirshfeld surfaces of molecules in the one dimensional chain in **2**. The electrostatic potential is mapped over the range +0.01 au (blue) to –0.01 au (red).

A search of the CSD,[21] resulted in a total of 176 single crystal structures incorporating HQ molecules. An additional search of recent literature revealed two further papers incorporating three additional structures.[22,23] Removing from these 179 structures all duplicates, measurements at different temperatures, re-interpretations, η^6 metal complexes, and structures with uncertain assignments of O–H protons or disordered protons on HQ, the 179 structures were reduced to 137. These structures include a total of 184 unique HQ molecules, for which 161 are in the *trans*-conformation (87.5%) and 23 in *cis*-conformation (12.5%). Interestingly, of the 7 HQ molecules in the co-crystals reported here, only one (14%) is in the *cis*-conformation. As pointed out by Oswald *et al*. the adoption of the centrosymmetric *trans*-conformer of HQ may be related to the general centrosymmetric packing in crystal structures, where the molecule has a tendency to occupy inversion centres.[24] Of the *trans*-conformers of the structures in the CSD, 128 (80%) lie on an inversion centre, which is in good agreement with the analysis of Pidcock *et al*., who showed that molecules with an inversion centre retained that symmetry element in the final crystal structure in 80% of the cases.[25] Similar preservation of symmetry is observed in crystal structures with other symmetry elements.

The *cis–trans* HQ isomerism has been studied by FTIR spectroscopy and DFT calculations by Akai *et al*., who found the *trans*-conformer to have only a slightly lower enthalpy than the *cis*-conformer, with a difference of only 0.56 kJ mol^{-1}.[26] The interconversion barrier between the two conformers was determined to be 10.8 kJ mol^{-1}. Given this small enthalpy difference it may be surprising that not more structures are found with HQ in the *cis*-conformation. The bias towards centrosymmetry can however be related to the promotion of more dense packing by crystallographic inversion centres.[24]

Conclusions

This study of three new HQ solvates underlines the way in which Hirshfeld surface and fingerprint plot analysis provides rapid quantitative insight into the intermolecular interactions in complex molecular solids. The close contacts of these solvates are dominated by H···H, C···H and H···C contacts, and these relatively weak interactions have clear signatures in the fingerprint plots. A correlation between H···C interactions and molecular volume appears to be observed, and the crystal packing and local density in the crystal is affected by these interactions.

The percentage of the HQ Hirshfeld surface volumes in each co-crystal appears to be correlated with the complexity of the 3-dimensional structure, with a low volume percentage being related to low-dimensional bonding. Even though **2** has a low volume percentage compared to **1** and **3**, it is the highest ever reported for a structure incorporating a *cis*-conformer of HQ. The preference of the *trans*-conformer is most likely due to the promotion of denser packing at the centrosymmetric inversions points, even though the energy difference between conformers is almost negligible.

Fast and easy calculation and visualization of properties on an isosurface of given molecular entities in solvates is possible, and this reveals that the hydrogen bonding pattern and the more subtle H···π interactions are accommodated by electrostatic complementarity.

Experimental

Synthesis

All solvents and starting materials were purchased from commercial suppliers and used without further purification. HQ was dissolved in the respective solvent and by slow evaporation of the solvent (propan-2-ol for **1**, *N*,*N*-dimethylacetamide for **2** and *N*,*N*-diethylformamide for **3**), single crystals of the respective co-crystals were obtained.

X-Ray crystallography

X-Ray diffraction data for compound **1** were measured on a single crystal at 100(2) K using an Oxford diffraction Xcalibur S system at the University of Western Australia, Perth.[27] Data were integrated, reduced and corrected for absorption using *CrysAlis RED*.[27] The data were scaled and merged using *SORTAV*.[28] The structure was solved by direct methods and subsequently refined against F^2 with *SHELX-97*.[30]

For compounds **2** and **3** data were collected at 100(2) K on a Bruker X8 APEX-II diffractometer at the Department of Chemistry, Aarhus University. Data were integrated using *SAINT+*.[31] The data of **2** were corrected for absorption and merged using *SORTAV*.[28] The data of **3** were corrected for absorption and merged with *SADABS*.[29] The structures were solved by direct methods and subsequently refined against F^2 with *SHELX-97*.[30]

Crystallographic information files for all structures were prepared using *enCIFer*[32] and *WinGX*,[33] and molecular graphics were prepared using *XShell*[34] and *CrystalExplorer*.[35]

In the refinements of **1**, **2** and **3** all non-H atoms were modeled with anisotropic atomic displacement parameters. The H atoms were placed on calculated positions and were subsequently allowed to ride on the parent atoms. The five highest residual peaks in **1** and ten highest residual peaks in **3** were located in the covalent bonding region of the molecules. In the structure of **2** unusual high residual peaks were located in the solvent region, which may be evidence of a small amount of disorder. Refinement of such disorder was unsuccessful, and further efforts at finding a better single crystal to obtain data of higher quality were also unsuccessful.

Crystal data and refinement details for **1**: $C_6H_6O_2$, C_3H_8O, M = 170.2, $F(000)$ = 184 e, triclinic, P-1 (no. 2), Z = 2, T = 100(2) K, a = 7.5561(5) Å, b = 8.1977(8) Å, c = 8.3331(6) Å, α = 88.322(7)°, β = 79.154(6)°, γ = 67.174(8)°, V = 466.71(7) Å^3, D_c = 1.211 g cm^{-3}, μ_{Mo} = 0.090 mm^{-1}, N_{unique} = 3191, $N_{measured}$ = 8574, R_{int} = 0.031, $N_{I > 2\sigma(I)}$ = 2117, $R(F^2 > 2\sigma(F^2))$ = 0.047, $wR(F^2)$ = 0.129, GOF = 1.41, ρ_{max} = 0.39 e/Å^3, ρ_{min} = –0.25 e/Å^3. CCDC 692266.

Crystal data and refinement details for **2**: $C_6H_6O_2$, C_4H_9NO, M = 197.23, $F(000)$ = 848 e, monoclinic, $C2/c$ (no. 15), Z = 8, T = 100(2) K, a = 11.1325(6) Å, b = 9.0410(5) Å, c = 21.0854(11) Å, β = 100.098(4)°, V = 2089.35(19) Å^3, D_c = 1.254 g cm^{-3}, μ_{Mo} = 0.092 mm^{-1}, N_{unique} = 3185, $N_{measured}$ = 27 651, R_{int} = 0.138, $N_{I > 2\sigma(I)}$ = 1791,

$R(F^2 > 2\sigma(F^2))$ = 0.062, $wR(F^2)$ = 0.162, GOF = 1.08, ρ_{max} = 0.59 e/Å^3, ρ_{min} = –0.33 e/Å^3. CCDC 692267.

Crystal data and refinement details for **3**: $2.5C_6H_6O_2$, $C_5H_{11}NO$, M = 376.42, $F(000)$ = 402 e, triclinic, P-1 (no. 2), Z = 2, T = 100(2) K, a = 5.5742(1) Å, b = 9.8776(3) Å, c = 17.6573(4) Å, α = 101.171(1)°, β = 92.245(2)°, γ = 99.443(2)°, V = 938.33(4) Å^3, D_c = 1.332 g cm^{-3}, μ_{Mo} = 0.098 mm^{-1}, N_{unique} = 7063, $N_{measured}$ = 28 368, R_{int} = 0.098, $N_{I > 2\sigma(I)}$ = 5086, $R(F^2 > 2\sigma(F^2))$ = 0.054, $wR(F^2)$ = 0.121, GOF = 1.03, ρ_{max} = 0.40 e/Å^3, ρ_{min} = –0.28 e/Å^3. CCDC 692268.

Computational

Electrostatic potentials on isosurfaces as well as dipole moments were computed using *ab initio* wavefunctions obtained from *Gaussian03*.[19] The calculations employed a MIDI! basis set at the Hartree–Fock level and molecular geometries were taken directly from the relevant crystal structures.

References

1 (*a*) G. R. Desiraju, *Nature*, 2001, **412**, 397–400; (*b*) K. Buhlmann, J. Reinbold, K. Cammann, K. Skobridis, A. Wierig and E. Weber, *Fresenius' J. Anal. Chem.*, 1994, **348**, 549–552.
2 (*a*) D. V. Soldatov, G. D. Enright, A. S. Zanina and I. E. Sokolov, *J. Supramol. Chem.*, 2002, **2**, 441–448; (*b*) G. R. Desiraju, *Comprehensive Supramolecular Chemistry*, 1996, vol. 6, (Solid-State Supramolecular Chemistry: Crystal Engineering), pp. 1–22.
3 G. R. Desiraju, in *Solid State Supramolecular Chemistry: Crystal Engineering*, ed. D. D. MacNicol, F. Toda and R. Bishop, Pergamon, Oxford, 1996, vol. 6, pp. 1.
4 M. A. Spackman and J. J. McKinnon, *CrystEngComm*, 2002, **4**, 378–392.
5 J. J. McKinnon, D. Jayatilaka and M. A. Spackman, *Chem. Commun.*, 2007, 3814–3816.
6 M. A. Spackman, J. J. McKinnon and D. Jayatilaka, *CrystEngComm*, 2008, **10**, 377–388.
7 H. M. Powell, *J. Chem. Soc.*, 1948, 61–73.
8 D. E. Palin and H. M. Powell, *J. Chem. Soc.*, 1948, 815–821.
9 D. E. Palin and H. M. Powell, *J. Chem. Soc.*, 1948, 571–574; T. C. W. Mak, *J. Chem. Soc., Perkin Trans. 2*, 1982, 1435–1437.
10 T.-L. Chan and T. C. W. Mak, *J. Chem. Soc., Perkin Trans. 2*, 1983, 777–781.
11 S. V. Lindeman, V. E. Shklover and Y. T. Struchkov, *Cryst. Struct. Commun.*, 1981, **10**, 1173–1179.
12 S. C. Wallwork and H. M. Powell, *J. Chem. Soc., Perkin Trans. 2*, 1980, 641–646.
13 J. J. McKinnon, M. A. Spackman and A. S. Mitchell, *Acta Crystallogr., Sect. B: Struct. Sci.*, 2004, **60**, 627–668.
14 A. Parkin, G. Barr, W. Dong, C. J. Gilmore, D. Jayatilaka, J. J. McKinnon, M. A. Spackman and C. C. Wilson, *CrystEngComm*, 2007, **9**, 648–652.
15 P. Munshi, B. W. Skelton, J. J. McKinnon and M. A. Spackman, *CrystEngComm*, 2008, **10**, 197–206.
16 L.-B. Lu, Y.-Q. Zhang, Q.-J. Zhu, S.-F. Xue and Z. Tao, *Molecules*, 2007, **12**(4), 716–722.
17 V. Blanco, M. Chas, D. Abella, E. Pia, C. Platas-Iglesias, C. Peinador and J. M. Quintela, *Org. Lett.*, 2008, **10**, 409–412.
18 P. Behmel and G. Weber, *J. Mol. Struct.*, 1984, **116**, 271–277.
19 M. J. Frisch, G. W. Trucks, H. B. Schlegel, G. E. Scuseria, M. A. Robb, J. R. Cheeseman, J. A. Montgomery, Jr., T. Vreven, K. N. Kudin, J. C. Burant, J. M. Millam, S. S. Iyengar, J. Tomasi, V. Barone, B. Mennucci, M. Cossi, G. Scalmani, N. Rega, G. A. Petersson, H. Nakatsuji, M. Hada, M. Ehara, K. Toyota, R. Fukuda, J. Hasegawa, M. Ishida, T. Nakajima, Y. Honda, O. Kitao, H. Nakai, M. Klene, X. Li, J. E. Knox, H. P. Hratchian, J. B. Cross, V. Bakken, C. Adamo, J. Jaramillo, R. Gomperts, R. E. Stratmann, O. Yazyev, A. J. Austin, R. Cammi, C. Pomelli, J. W. Ochterski, P. Y. Ayala, K. Morokuma, G. A. Voth, P. Salvador, J. J. Dannenberg, V. G. Zakrzewski, S. Dapprich, A. D. Daniels, M. C. Strain, O. Farkas, D. K. Malick, A. D. Rabuck, K. Raghavachari, J. B. Foresman, J. V. Ortiz, Q. Cui, A. G. Baboul, S. Clifford, J. Cioslowski, B. B. Stefanov, G. Liu, A. Liashenko, P. Piskorz, I. Komaromi, R. L. Martin, D. J. Fox, T. Keith, M. A. Al-Laham, C. Y. Peng, A. Nanayakkara, M. Challacombe, P. M. W. Gill, B. Johnson, W. Chen, M. W. Wong, C. Gonzalez and J. A. Pople, *GAUSSIAN 03, (Revision C.02)*, Gaussian Inc., Wallingford CT, 2004.
20 W. Caminati, S. Melandri and L. B. Favero, *J. Chem. Phys.*, 1994, **100**, 8569–8572.
21 F. H. Allen and W. D. S. Motherwell, *Acta Crystallogr., Sect. B: Struct. Sci.*, 2002, **58**, 407–422, CSD version 5.30 (Nov. 2008 incl. the Feb. 2009 update).
22 D. R. Weyna, T. Shattock, P. Vishweshwar and M. J. Zaworotko, *Cryst. Growth Des.*, 2009, **9**(2), 1106–1123.
23 T. M. Polyanskaya and K. A. Khaldoyanidi, *J. Struct. Chem.*, 2008, **49**(2), 327–334.
24 I. D. H. Oswald, W. D. S. Motherwell and S. Parsons, *Acta Crystallogr., Sect. B: Struct. Sci.*, 2005, **61**, 46–57.
25 E. Pidcock, W. D. S. Motherwell and J. C. Cole, *Acta Crystallogr., Sect. B: Struct. Sci.*, 2003, **59**, 634–640.
26 N. Akai, S. Kudoh, M. Takayanagi and M. Nakata, *Chem. Phys. Lett.*, 2002, **356**, 133–139.
27 *CrysAlis* CCD and *CrysAlis* RED, version 1.171.32.5 (release 08-05-2007 CrysAlis171.NET) Oxford Diffraction Ltd., Abingdon, Oxfordshire, UK.
28 SORTAV, R. H. Blessing, *Crystallogr. Rev.*, 1987, **1**, 3–58; R. H. Blessing, *J. Appl. Crystallogr.*, 1989, **22**, 396–397.
29 G. M. Sheldrick, *Program for Scaling and Absorption Correction*, University of Göttingen, Göttingen, 1997. SADABS.
30 G. M. Sheldrick, *SHELXS97, Program for Crystal Structure Solution*, University of Göttingen, Göttingen, 1997; G. M. Sheldrick, *SHELXL97, Program for Crystal Structure Refinement*, University of Göttingen, Göttingen, 1997.
31 Bruker, *APEX2* and *SAINT-Plus*, Bruker AXS Inc., Madison, Wisconsin, USA, 2004.
32 enCIFer: A program for viewing, editing and visualising CIFs. F. H. Allen, O. Johnson, G. P. Shields, B. R. Smith and M. Towler, *J. Appl. Crystallogr.*, 2004, **37**, 331–334.
33 WinGX: L. J. Farrugia, *J. Appl. Crystallogr.*, 1999, **32**, 837–838.
34 Xshell V.4.02: Graphical interface for crystal structure refinement, Bruker AXS, Madison, Wisconsin, USA, 2000.
35 S. K. Wolff, D. J. Grimwood, J. J. McKinnon, D. Jayatilaka and M. A. Spackman, *Crystal Explorer V. 2.0.0 alpha (r367)*, University of Western Australia, 2005–2007.